Astron. Astrophys. 54, 841—851 (1977)

ASTRONOMY
AND
ASTROPHYSICS

Ultraviolet Photometry with the Astronomical Netherlands Satellite ANS: A Study of the Surface Brightness of the Merope Reflection Nebula

C. D. Andriesse[1], Th. R. Piersma[1] and A. N. Witt[2]

[1] Kapteyn Astronomical Institute, University of Groningen
[2] Laboratory for Atmospheric and Space Physics, University of Colorado and Ritter Astrophysical Research Center, The University of Toledo, Ohio 43606, USA

Received June 18, 1976

Summary. New measurements of the surface brightness of the Merope reflection nebula in 14 positions at the wavelengths 1550, 1800, 2200, 2500 and 3300 Å are reported. These are shown to form a set of data entirely consistent with existing ground-based observations of the same nebula at $\lambda\lambda$ 3400, 4110, 4630 and 5620 Å by O'Dell, thus extending the frequency base by a factor of three. The nebular colour near the illuminating star 23 Tau is found to be bluer than that of the star over the entire wavelength range, but at greater angular distances the nebular colour is substantially redder than that of the star. The surface brightness distribution as function of angular distance from the illuminating star can be fitted to high accuracy to a power law. The value of the exponent decreases smoothly from -1.5 at 1550 Å to -0.5 at 5620 Å.

The observational results are qualitatively compared with multiple scattering models for plane-parallel nebulae computed by the Monte Carlo technique. It is found that the illuminating star is most likely located in front of the nebula with respect to the observer. The nebular plane appears to be inclined with respect to the plane of the sky by an angle exceeding 50°. Several different aspects of the observations can be understood only if the phase function of the scattering particles changes from a strongly forward scattering form at visible wavelengths to a more nearly isotropic form at 1550 Å. No firm conclusions concerning albedo variations can be drawn, but the surface brightness observed suggests that the albedo is relatively high at all wavelengths studied.

Key words: reflection nebula — ultraviolet surface brightness — scattering properties of grains

I. Introduction

The bright reflection nebula near Merope (23 Tau) is of interest for a study of the optical properties of dust grains. Its structure and position with respect to the star are not too uncertain, so that one can hope to separate geometrical effects from grain effects. This motivated O'Dell (1965) and Elvius and Hall (1966) to conduct photometric and polarimetric studies of various regions of the nebula. Subsequently Greenberg and Hanner (1970) interpreted the data in terms of dielectric grains. It is of interest to extend the observations into the ultraviolet, where the interstellar extinction (Savage, 1975) suggests other grains absorbing around 2200 Å and efficiently scattering shortward of 1500 Å (Witt and Lillie, 1973; Lillie and Witt, 1976).

The ultraviolet photometer on board of the Astronomical Netherlands Satellite ANS (van Duinen et al., 1975) enabled such observations because of its sensitivity, offset pointing mode and modest (2.5′ square) field of view. In February and August 1975 we observed 14 regions in the nebula through narrow band filters at 1550, 1800, 2200, 2500 and 3300 Å. A quantitative analysis of the data will take some time, because variants of the likely geometry have to be considered. Furthermore, the optical depth of the nebula must reach rather substantial values in the ultraviolet. Consequently, photons are certainly scattered more than once before escaping from the nebula, so that a relatively simple analysis based on single scattering alone would be misleading. The position of the star with respect to the nebula, while most critical in a single scattering analysis, still remains a very important model parameter in multiple scattering studies and must therefore remain a subject of further inquiry. In this paper we report on the observations themselves and give a qualitative discussion of the possible geometry and grain properties. It is expected that this investigation will be followed by a more exhaustive quantitative study at a later time.

II. Observations

1. Procedure and Reductions

The 14 observed regions of the reflection nebula are indicated on Figure 1 (together with those by O'Dell) and the central co-ordinates are given in Table 1 (their

Send offprint requests to: C. D. Andriesse

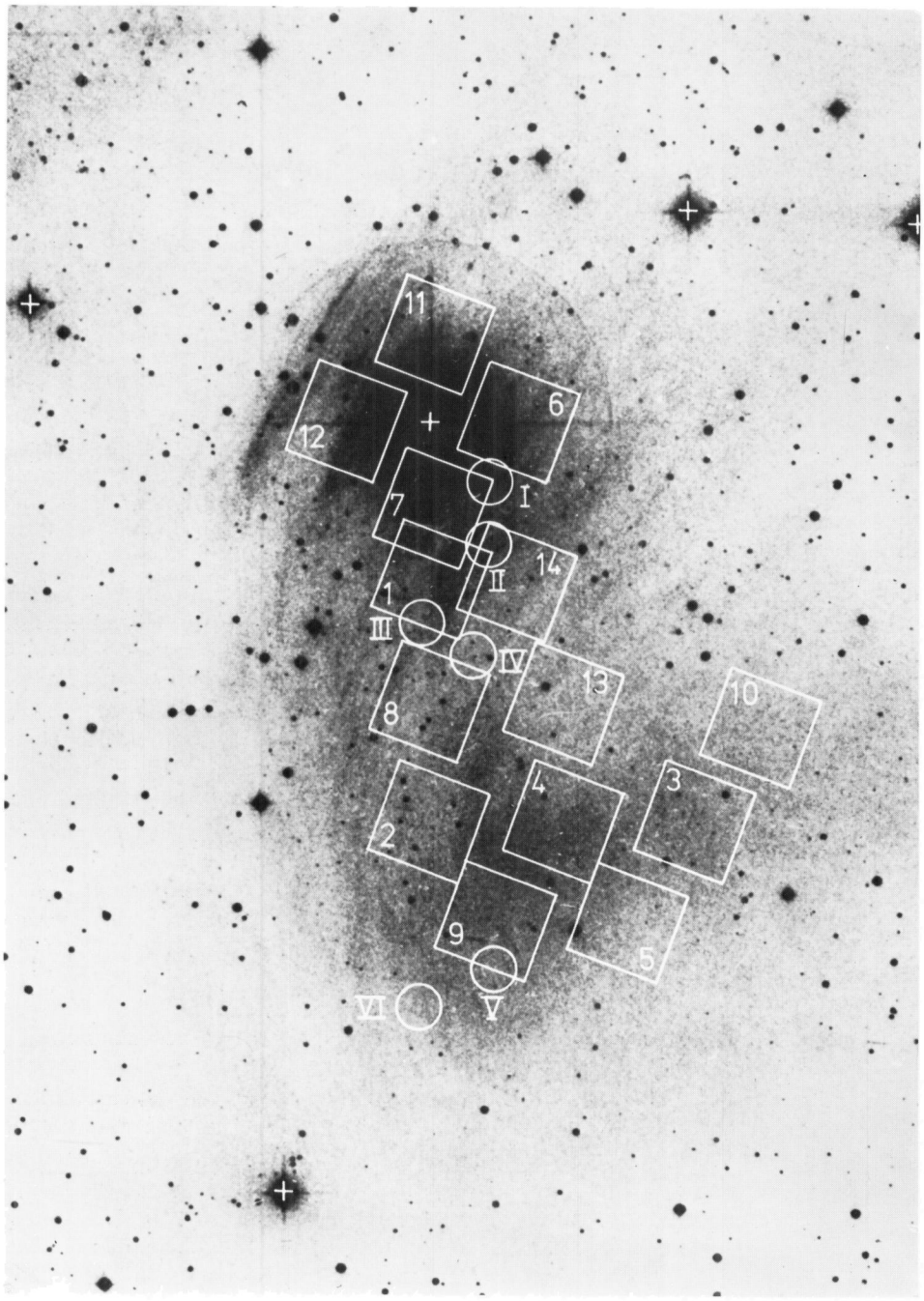

Fig. 1. The Merope nebula as reproduced from the red print of the *Palomar Observatory Sky Survey*. The square regions observed by ANS, numbered 1–14, are 2.5 × 2.5 in size. The circular regions, numbered I–VI, are those observed by O'Dell (1965)

accuracy is $\pm 0.4'$). We quote them by the priority number in the satellite's observing programme. The first 5 positions were measured on 1975, February 19 on a trial basis. They were repeated and extended by another 9 positions on 1975, August 22 and 23, when we intended to cover much of the measurable parts of the nebula. The regions do not contain stars brighter than $m_v = 10$. We obtained 2 independent pointings on region 6; 4 on 7, 8, 9, 10, 11, 13, 14; 6 on 5, 12 and 7 on 1, 2, 3, 4. Merope was included 9 times. Each observation consisted of a small sequence of measurements of the object and the background.

Because of the extended nebulosity of the Pleiades in general and its numerous stars the normal offset procedure for measuring an "empty sky" was abandoned. Instead we measured the dark current. This is induced by the Earth's radiation belts and therefore depends on the position of the satellite in its orbit. In particular for the 3300 Å channel the variation in this current was important. Furthermore, it is induced by a calibration

Table 1. Central positions of observed regions

No.	R.A. (1950)	DEC (1950)
1	$3^h43^m21^s$	23°43′39″
2	3 43 21	23 37 39
3	3 42 51	23 37 39
4	3 43 06	23 37 40
5	3 42 58	23 35 10
6	3 43 11	23 47 39
7	3 43 21	23 45 24
8	3 43 21	23 40 39
9	3 43 13	23 35 09
10	3 42 44	23 40 09
11	3 43 21	23 49 54
12	3 43 31	23 47 39
13	3 43 06	23 40 39
14	3 43 11	23 43 39

source of Čerenkov radiation, which does not affect the proper ultraviolet measurements. In measuring the "empty sky" the latter effect is replaced by the current due to the diffuse zodiacal and galactic light. The difference between these two has been studied by de Boer and Koornneef (1975) for various regions of the sky and is found to be rather constant. Therefore, measurements of the dark current give, when corrected with this difference, a fair estimate of the background. We have subtracted the background using either a linear or a quadratic interpolation formula fitted to the sequence of measurements. Absolute fluxes are then obtained using the adjusted calibration of the photometer (Wesselius, 1975) and the orbit efficiency (Aalders, 1976). The statistical accuracy in the stellar flux is about 0.5% for each wavelength band. For the nebular regions we will not quote individual errors because of the difficulty to combine the poor statistics of the counts and the different pointings. However, the complete set of data appears to be internally consistent, which suggests a reasonable accuracy with probable errors of the order of 10% and less. Absolute fluxes for 23 Tau are listed in Table 3 and nebular surface brightnesses relative to the flux from 23 Tau are presented in Table 4.

2. *The Stellar Spectrum*

Let us comment first on the spectrum of Merope (23 Tau) itself. The star is classified as B 6 IV *nn* with a colour excess $E(B-V)=0.084$. Extinction in its spectrum is evident in Figure 2. In Table 2 we present data on the average interstellar extinction, based on ANS observations and in close agreement with determinations by earlier satellites, and the corresponding extinction factors for the flux from Merope. With these factors we have corrected the observed flux and compare this with fluxes from three essentially unreddened B 6 V stars (Table 3). Normalising the fluxes of the latter at 2500 Å to $30.2\,10^{-11}$ erg s^{-1} cm^{-2} Å^{-1} and averaging them we get the full curve in Figure 2. The corrected fluxes from Merope fit this curve very well at the longer wavelengths,

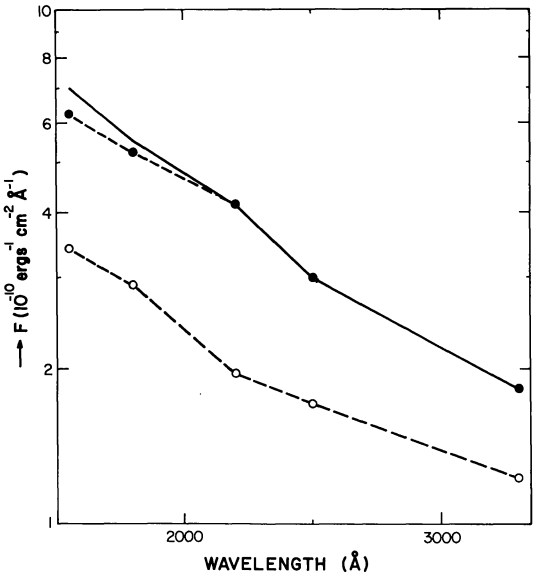

Fig. 2. The ultraviolet energy distribution of 23 Tau as observed by ANS (--○--) and after correction for average interstellar extinction (--●--). The solid line represents the average of the normalized spectrum of three essentially unreddened B 6 V stars observed by ANS

Table 2. ANS data on the average interstellar extinction A and the extinction toward Merope, where $E(B-V)=0.084$ mag ($A=1.0857\tau$)

λ [Å]	$\frac{A-A(3300)}{E(B-V)}$	23 Tau	
		A	$\exp(-\tau)$
1550	2.63	0.654	0.547
1800	2.51	0.644	0.553
2200	4.64	0.823	0.469
2500	2.12	0.612	0.569
3300	0	0.433	0.671
4300	−1.04	0.346	0.727
5500	−2.04	0.262	0.786

Table 3. Fluxes from 23 Tau as observed and corrected for interstellar extinction, and from three unreddened B 6 V stars (courtesy C. C. Wu). Units: 10^{-11} erg s^{-1} cm^{-2} Å^{-1}

λ [Å]	23 Tau		HD		
	Obs.	Corr.	39844	81848	90994
1550	34.2	62.5	23.42	31.28	27.87
1800	29.1	52.6	19.36	24.98	22.09
2200	19.57	41.7	14.74	18.39	16.57
2500	17.16	30.2	10.74	13.00	12.11
3300	12.39	18.5	6.73	7.55	7.31

but at the shorter wavelengths the applied correction falls short. This cannot be ascribed to the minor difference in luminosity class between Merope and the comparison stars. One recalls the possibility (Maeder, 1975) that the flux deficiency at the shorter wavelengths of about 0.1 mag is caused by the rapid rotation of Merope with $v \sin i = 294$ km s^{-1}. Even the observed spread in the ultraviolet interstellar extinction curve from star to star can allow for the observed difference

between the corrected spectrum of Merope and that of the reference stars. In the absence of clear circumstellar effects (Code, 1973), one cannot infer that the star is immersed in the nebula. Fesenkov (1955) and O'Dell (1965) have argued that the star is just in front of the nebula. For this geometry Greenberg and Hanner (1970) could not match the then known colour-offset angle dependence for the nebula with any reasonable grain model, using a single scattering approach. Their most satisfactory fit required the star to be immersed in the nebula by a distance corresponding to a colour excess $E(B-V)=0.13$ for 23 Tau, which is in conflict with the reddening actually observed. It is hoped that an adequate multiple scattering treatment can remove these conflicts. We shall return to this question.

3. *Comparison with Ground-Based Measurements*

The surface brightness observations of the Merope Nebula by O'Dell (1965) at the wavelengths 3400, 4110, 4630 and 5620 Å appear to be most suitable for comparison with the present data for several reasons. The range of angular distances covered and portions of the nebula observed are nearly identical with parts of our data and O'Dell's shortest wavelength filter nearly agrees with the longest wavelength bandpass in our program both in width and central wavelength. To facilitate a direct comparison, all measurements are converted to units of $\log[S/F]_\lambda$, where S is the surface brightness of the nebula per steradian, $(206265)^2$/(area in square arc s) $\times F_N$, where F_N is the flux from the nebular region, and F is the flux from 23 Tau received at the Earth, both at the same wavelength λ. The current data in this form, together with the appropriate field numbers and angular distances from the central star in arc seconds, are listed in Table 4. O'Dell's results, reduced to the same format, are contained in Table 5.

In Figure 3 we show the ANS data of the surface brightness as a function of the distance to the star. The data at 3300 Å are displayed together with O'Dell's data at 3400 Å. Considering that the field positions and sizes differ in the two programs and that the surface brightness distribution of the Merope nebula does exhibit some patchiness, the agreement is good. We will therefore consider the data at 3300 Å and 3400 Å together, despite the fact that they apply to different regions and different diaphragms.

4. *Surface Brightness Distribution and Nebular Colour*

As is apparent from Figure 3, the surface brightness of the Merope nebula varies smoothly with angular distance from the illuminating star. We have carried out a least squares fit of the surface brightness distributions observed by ANS and by O'Dell (1965) to an expression

$$S/F \propto r^p \qquad (1)$$

where r is the angular distance from the illuminating star in arc seconds. In the log-log representation of Figure 3,

Table 4. Relative surface brightness distribution of the Merope reflection nebula observed by ANS

Position	r ["]	$\log(S/F)$				
		λ 1550	λ 1800	λ 2200	λ 2500	λ 3300
7	135	4.263	4.225	4.158	4.132	4.054
11	135	4.128	4.104	4.048	4.002	3.909
6	137	4.134	4.121	4.064	4.058	3.985
12	137	4.094	4.059	4.012	3.985	3.900
1	240	3.881	3.857	3.822	3.826	3.821
14	277	3.718	3.672	3.615	3.616	3.672
8	420	3.523	3.511	3.499	3.550	3.638
13	468	3.391	3.379	3.347	3.355	3.466
2	600	3.222	3.285	3.274	3.344	3.447
4	634	3.127	3.181	3.175	3.237	3.412
10	679	3.106	3.123	3.090	3.165	3.344
3	728	3.013	3.029	3.041	3.142	3.331
9	758	3.002	3.077	3.059	3.130	3.323
5	814	2.909	2.947	2.957	3.060	3.309

Table 5. Relative surface brightness distribution of the Merope reflection nebula observed by O'Dell (1965)

Position	r ["]	$\log(S/F)$			
		λ 3400	λ 4110	λ 4630	λ 5620
I	127	4.065	4.018	3.954	3.849
II	210	3.896	3.869	3.822	3.739
III	304	3.759	3.770	3.743	3.656
IV	358	3.606	3.646	3.626	3.580
V	832	3.258	3.446	3.481	3.528
VI	885	3.054	3.301	3.318	3.360

we demonstrate the closeness of such fits to the ANS data. The power p, equal to the slopes of the straight lines in Figure 3, was determined for O'Dell's data as well and is plotted in Figure 4 as a function of wavelength. The uncertainty in the values of p is about ± 0.10 for the ANS data and somewhat larger in O'Dell's data, because fewer regions are involved here. Within that uncertainty we find a smooth decrease from $p \simeq -1.5$ at 1550 Å to $p \simeq -0.5$ at 5620 Å. As will be shown later, this observed range of p is unusually large and can be understood only under rather special circumstances involving the star-nebula geometry and the scattering properties of the nebular particles.

The representation of the surface brightness distributions at different wavelengths by a power law given by Equation (1) permits us to determine the nebular surface brightness for fixed angular distances even though different fields were observed by ANS and in the O'Dell study. In Figure 5 we show the quantity $\log(S/F)$ extrapolated to angular distances of 100″ and 800″ as a function of wavelength. It appears that close to the star at 100″ the surface brightness relative to the stellar flux increases with decreasing wavelength, which means that the nebular colour is consistently bluer than that of the star throughout the spectral range covered. On the other hand, at 800″ radial distance, the surface brightness

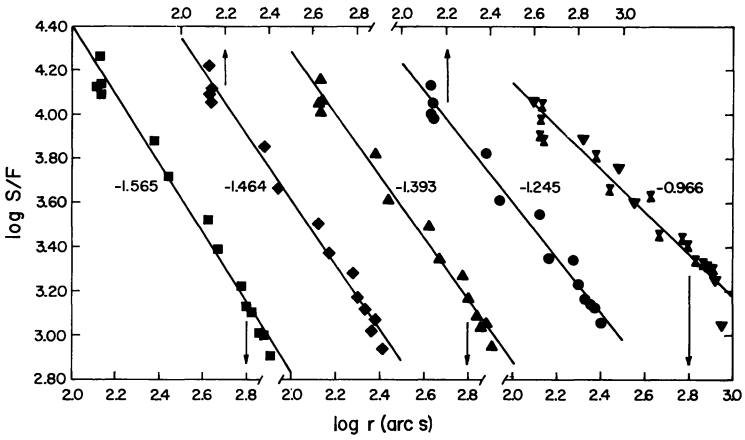

Fig. 3. Surface brightness versus angular distance from the star at 1550 Å (■), 1800 Å (◆), 2200 Å (▲), 2500 Å (●), 3300 Å (⧗) and 3400 Å (▼). The straight lines indicate fits to Equation (1) and the parameters indicate the values of p

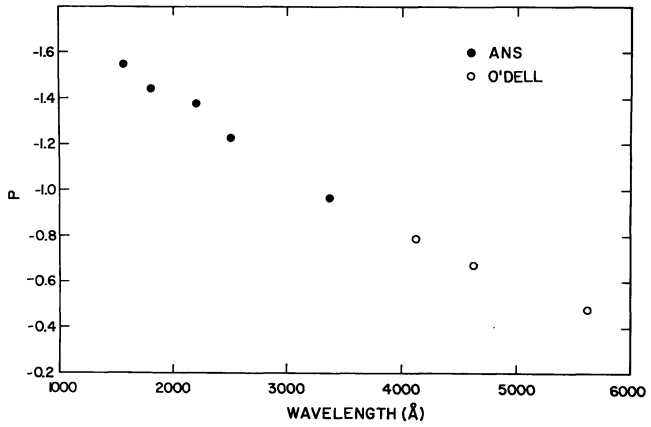

Fig. 4. The exponent of the surface brightness power law as a function of wavelength

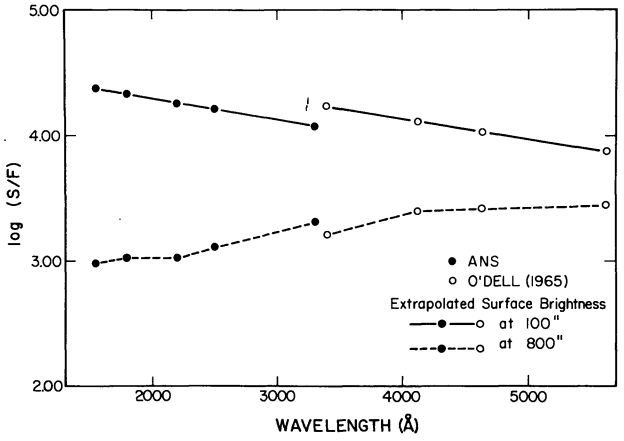

Fig. 5. The extrapolated relative surface brightness at the angular distance of 100″ and 800″ from the illuminating star 23 Tau, as a function of wavelength

decreases with decreasing wavelength, indicating that the nebula is redder here than the illuminating star. The junctions at λ 3300/3400 Å are not perfect, which is due in part to the fact that different field locations have been measured for the two halves of the graph. In addition, it is possible that small differences in the sky background correction employed and in the vignetting in the two observing systems contributed to the lack of continuity. It is very important, however, that at λ 3300/3400 Å there exists a continuity of slope, which should permit us to carry out a parallel translation in order to determine the total range of $\log(S/F)$ at 100″ and 800″ between the wavelengths 5620 Å and 1500 Å. In this manner we find at 100″ that $\log(S/F)_{1550} - \log(S/F)_{5620} = +0.66$ and at 800″ that $\log(S/F)_{1550} - \log(S/F)_{5620} = -0.56$. A successful model for the Merope nebula must explain these values as well as their opposite sign.

The change of nebular colour relative to that of the star occurs smoothly with increasing radial distance. In Figure 6 the quantity $\log(S/F)$ has been normalized to zero at 3300 Å and plotted as function of wavelength shortward of 3300 Å for all individual 14 ANS fields. Positive values of $\log(S/F)_\lambda - \log(S/F)_{3300}$ indicate blue relative colour, negative values red relative colour. It is apparent from Figure 6 that the change from blue to red for the wavelength interval from 3300 Å to 2200 Å happens in the vicinity of field No. 1 and No. 14, corresponding to an angular distance of about 250″ from 23 Tau. Dahn (1967), by combining results from several ground-based studies of the Merope nebula, finds this colour neutrality to occur around 500″ for the colour difference in $(B-V)$ and around 390″ for the colour difference in $(U-B)$. Our result appears to continue this trend with an even closer point of colour neutrality as we proceed from 3300 Å to 2200 Å.

It is also noteworthy that the colour changes become relatively weak with change in position, when one considers the spectral range 2200 Å to 1550 Å. For this wavelength interval the point of colour neutrality has moved out to $r \simeq 600''$. This may be indicative of distinct changes in the variation of optical depth, the albedo and the phase function with wavelength as one proceeds shortward of λ 2200 Å.

III. A Qualitative Interpretation

1. Models for Reflection Nebulae

Past attempts to quantitatively explain observations of reflection nebulae have met with only limited success. The problem has been reviewed in depth by Dahn (1967)

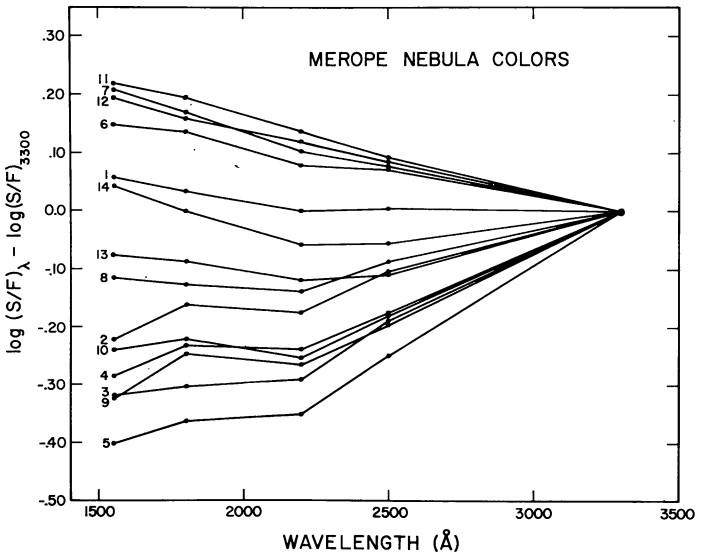

Fig. 6. The ultraviolet colours of the Merope nebula normalized at 3300 Å. The number at the left of each line refers to the position number. Positive values on the ordinate indicate nebula colours bluer than the star's colours

and Vanysek (1969). The nature of the difficulty lies in the fact that the complete description of the star-nebula system including the scattering properties of the nebular particles requires substantially more parameters than are generally available from independent observations. In addition, the radiative transfer treatments which have been applied to the reflection nebula problem in the past have been largely limited to considerations of single scattering only, an approach of doubtful validity in light of the significant optical thickness of most bright reflection nebulae and the high albedo of interstellar grains. This inadequacy would become even more severe in the analysis of ultraviolet observations, where the nebular optical thickness is typically two to three times as large as the value at visible wavelengths. In Figure 7 we demonstrate this fact by showing the average number of scatterings experienced by a photon as a function of the angular distance of the exit position to the star. The multiplicity of scattering is seen to increase substantially with increasing angular distance and optical thickness of the nebula. The results shown in Figure 7 have been obtained from Monte Carlo studies of the radiative transfer in plane-parallel nebulae.

This practical approach to the transfer problem has been successfully demonstrated by Roark et al. (1974), who used the Monte Carlo technique to treat multiple scattering in a plane-parallel cylindrical geometry with a star outside the nebula. The method has been further developed by one of us (A.N.W.) and the details of this very extensive radiative transfer study will be reported elsewhere (Witt, 1976). Here, we shall quote only those results which are of use in understanding the Merope data presented here and which can be qualitatively justified.

2. *Model Assumptions*

The most significant aspect of the problem in which an initial assumption must be made is the star-nebula geometry. Fesenkov (1955) and Vanysek (1969) have suggested that a plane-parallel nebula model is the most suitable description of the Merope Nebula. This is supported by the large angular extent of the object over which the line of sight optical depth appears to be fairly constant, based on the number of visible background stars. This optical depth is generally assumed to be of order unity at λ 5500 Å based on Mendoza's (1965) study of the star HD 23512, which is located apparently behind the Merope nebulosity. The colour excess for this star is $E(B-V)=0.36$. By contrast, the colour excess of 23 Tau is only $E(B-V)=0.084$, which has led Fesenkov (1955) and O'Dell (1965) to conclude that 23 Tau is located in front of the nebula as seen by the observer and that its reddening is interstellar in nature. This is also suggested by the very gentle decrease in nebular surface brightness at visible wavelengths with angular distance from 23 Tau. It can only be understood with the star in front of the nebula, if the scattering properties of the dust particles in this spectral region are characterized by an albedo near 0.7 and a strongly forward throwing phase function (Mattila, 1970; FitzGerald et al., 1976). This conclusion is substantiated by the results of model calculations where multiple scattering has been included. In Figure 8 we present calculations for the variation of log (S/F) with angular distance for a plane-parallel nebula of 1 pc thickness and an optical thickness of 1.3. Greenberg and Hanner (1970) suggested that the star should be embedded into the nebula by a distance of 0.35 pc and the scattering grains should be dielectric. We can approximately describe such grains by an albedo $a=0.65$ and a phase function asymmetry $g=0.75$. The two curves indicating a very steep brightness decrease are found for cases where the star is embedded by 0.10 pc and 0.50 pc, respectively, thus bracketing the location suggested by Greenberg and Hanner (1970). The third curve displaying a much more gradual decrease in the surface brightness results for a star location at 0.05 pc in front of the nebula. All three models were calculated for a tilt of 10° of the nebular plane with respect to the

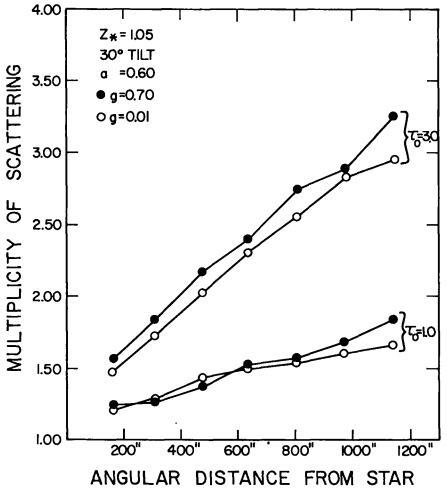

Fig. 7. Monte Carlo model calculations: The average number of scatterings experienced by photons seen by the observer at various angular distances from the star. Cases of $\tau_0=1$ and $\tau_0=3$ are demonstrated for the cases of a strongly forward throwing phase function ($g=0.7$) and a nearly isotropic phase function ($g=0.01$). The star is located 0.05 pc in front of a plane-parallel nebula of 1 pc thickness

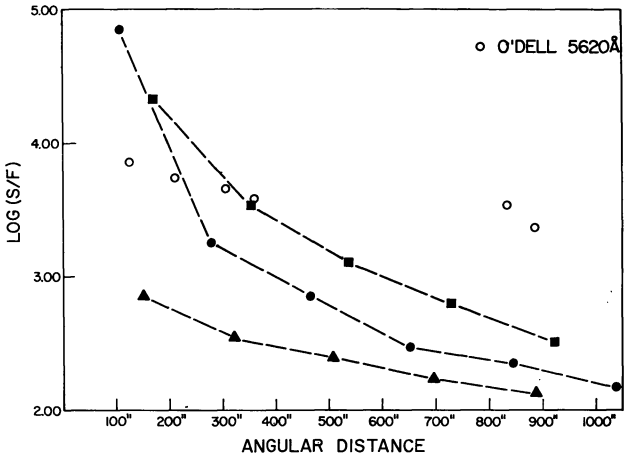

Fig. 8. Monte Carlo model calculations: The surface brightness distribution for a plane-parallel nebula of 1 pc thickness and $\tau_0=1.3$. The particles have an assumed albedo $a=0.65$ and a phase function asymmetry $g=0.75$. The star's position is 0.5 pc below the front surface (■), 0.1 pc below the front surface (●), and 0.05 pc in front of the nebula (▲). For comparison O'Dell's observations (○) at 5620 Å are shown

plane of the sky as suggested by Greenberg and Hanner (1970). For comparison, the nebular surface brightness measurements at 5620 Å by O'Dell (1965) are shown. While none of the three models fit the data particularly well, it appears that only the case with the star in front of the nebula can produce the gentle decrease of the surface brightness with distance which is observed. For the following discussion we shall, therefore, assume that 23 Tau is in front of the nebula. No further assumptions will be made with respect to its distance from the front surface, with respect to the physical thickness of the nebula, or the tilt of the nebular plane with respect to the plane of the sky.

For the distance of the Merope Nebula we assume $d=126$ pc in accordance with Allen (1973). We assume that the scattering properties of the nebular dust grains can be described by the values of the single scattering albedo, a, and the asymmetry, g, of the Henyey-Greenstein phase function (Henyey and Greenstein, 1941):

$$\Phi(\alpha)=[(1-g^2)/4\pi](1+g^2-2g\cos\alpha)^{-3/2}. \quad (2)$$

All models for which results will be discussed here are based on Monte Carlo studies involving $3\,10^6$ photons in each case. The design of the models is such that predicted surface brightness values have an uncertainty of $\pm 3\%$, based on photon statistics. Complete multiple scattering is taken into account. It will be assumed that the wavelength dependence of the nebular optical thickness into the ultraviolet is generally the same as that of the average interstellar extinction (Table 2, Bless and Savage, 1972).

3. *Model Results*

In Figure 9 we display the calculated quantity $\log(S/F)$ as a function of optical thickness of the nebula for two values of the phase function asymmetry and for two values, 100″ and 800″, of angular distance from the star. A nearly isotropic phase function is represented by $g=0.01$, while $g=0.70$ is typical for a strongly forward throwing phase function. The physical thickness of the plane-parallel layer is taken to be 1 pc which we estimate to be the correct order of magnitude, and the distance of the star from the front surface was chosen as 0.05 pc. These parameters will be kept at these values arbitrarily, since it is our principal aim to study the qualitative effects of tilt changes and the variations of optical depth, albedo and phase function with wavelength.

The tilt angle, θ, by which we will refer to the angle between the nebular plane and the plane of the sky, was held at 10° for the models in Figure 9. To obtain line of sight values of the optical thickness, we must multiply the values of τ_0, the optical thickness along the nebular axis, by $(\cos\theta)^{-1}$.

Since the optical depth between 5620 and 2200 Å increases by a factor of ~ 3.1, the increase in observed relative surface brightness at 100″ as shown in Figure 5 can be explained to first order as an optical depth effect, as demonstrated in Figure 9. The fact that the observed values of $\log(S/F)$ are reproduced approximately only by the case for $g=0.01$ should be of no concern, since the vertical position of the displayed curves can be changed easily by changing the value of the albedo a (here taken to be 0.60), the distance of the star from the front surface, or the physical thickness of the nebula. The observed $\log(S/F)$ curve for 100″ in Figure 5 continues to rise shortward of 2200 Å although the optical depth is likely to decrease. This can be understood only if a increases or g decreases shortward of 2200 Å, or if a combination of both occurs.

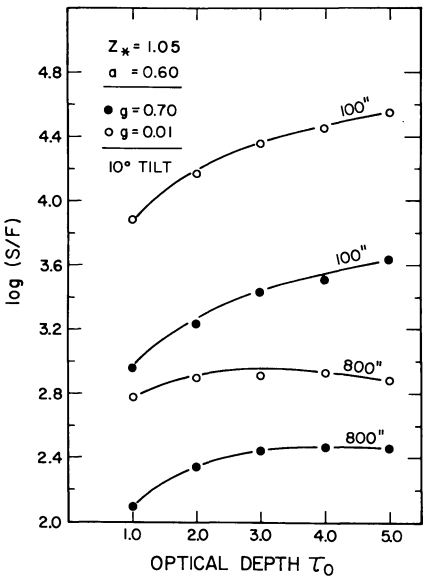

Fig. 9. Monte Carlo model calculations: Relative surface brightness at angular distances 100″ and 800″ is calculated as function of optical depth for a plane-parallel nebula. The illuminating star is located in front of the nebula at a distance of 0.05 pc. Solutions for a phase function asymmetry $g=0.70$ and $g=0.01$ are indicated for particles with an albedo $a=0.60$

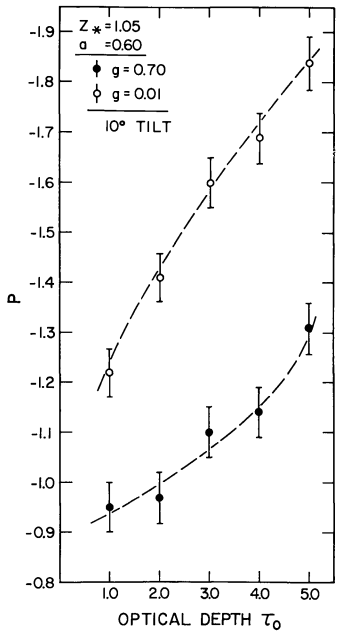

Fig. 10. Monte Carlo model calculations: The exponent of the surface brightness power law is plotted as function of optical depth for the same models as Figure 9

An apparent contradiction between models and observation occurs when we examine log (S/F) at 800″. Most models predict that with increasing optical thickness into the ultraviolet $\log(S/F)$ should increase also at 800″ when progressing from 5620 to 2200 Å, while a substantial decrease is actually observed. This trend, already observable between 5620 and 3400 Å, led O'Dell (1965) to suggest that a phase function variation with wavelength contributes to the observed nebular reddening. We shall demonstrate that this must indeed be the case.

Before progressing to this point, let us consider the shape of the surface brightness distribution with decreasing wavelength or increasing optical depth. The calculated values of $\log(S/F)$ versus angular distance for the distance interval from 100″ to 900″ can be fitted to power laws to a closeness exceeding that demonstrated in Figure 3. In Figure 10 we have plotted the power p for the models displayed in Figure 9. It is apparent that at least part of the observed change in p with wavelength in Figure 4 can be explained by the increase in optical depth to shorter wavelength. But it is also clear that the range of $\Delta p \simeq 1$ between 1550 and 5620 Å is not nearly reproduced, nor do we reach values of $p \simeq -0.5$ at an optical depth near unity.

Under what set of circumstances involving the geometry and the scattering properties as function of wavelength can we simultaneously increase the range of p and have the surface brightness at 800″ decline with increasing optical depth, while the surface brightness at 100″ increases with increasing optical depth? The answer emerges from Figure 11 where we consider a model for $\tau_0=3$ for a wide range of tilt angles and where the quantity $\log(S/F)$ is determined on the radius inclined towards the observer. It should be emphasized that the same qualitative behavior as seen here is found for other choices of the optical depth as well.

As the tilt angle is increased, the relative surface brightness at 100″ angular distance rises also. This is primarily due to the rise in $\tau_0/\cos\theta$. For $g=0.70$ an additional increase is caused by the fact that the effective scattering angle at 100″ becomes sufficiently far removed from 180°, so that the increase in the phase function for scattering angles less than 180° becomes important. Therefore, the rate of increase in $\log(S/F)$ at 100″ is greater for $g=0.70$ than for $g=0.01$, where such a phase function advantage does not exist. Due to combined projection and foreshortening effects the physical location of the 100″ point changes hardly at all. At the larger distance of 800″, however, the relative surface brightness of $g=0.01$ declines noticeably for a large tilt. While the optical depth still increases linearly with $(\cos\theta)^{-1}$, the illumination of the 800″ point decreases quadratically with $\cos\theta$, resulting from the increasing physical distance to the star when the same angular distance is maintained and the tilt increased. For $g=0.7$ one additional effect enters. The forward directed part of the phase function contributes more and more of the scattered light seen by the observer, and this more than overwhelms the effect of the increased distance in the range of tilts considered. Therefore, there exists a critical tilt angle, here about 50°, above which the surface brightness at 100″ will increase as one proceeds from a forward scattering phase function with $g=0.70$ to a more isotropic case of $g=0.01$, while there will be a

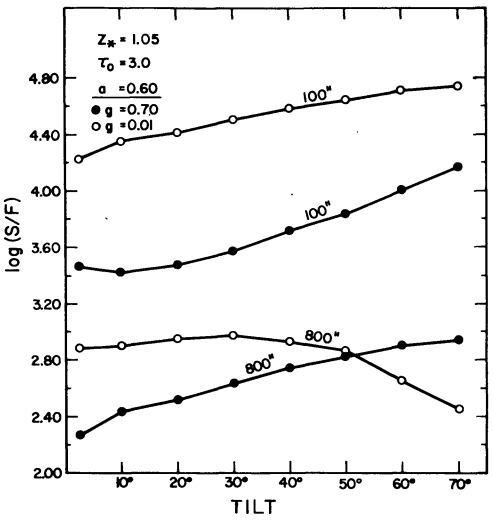

Fig. 11. Monte Carlo model calculations: Relative surface brightness at 100″ and 800″ angular distance as function of tilt angle between the nebular plane and the plane of the sky. A specific optical depth of $\tau_0 = 3$ is chosen for illustration

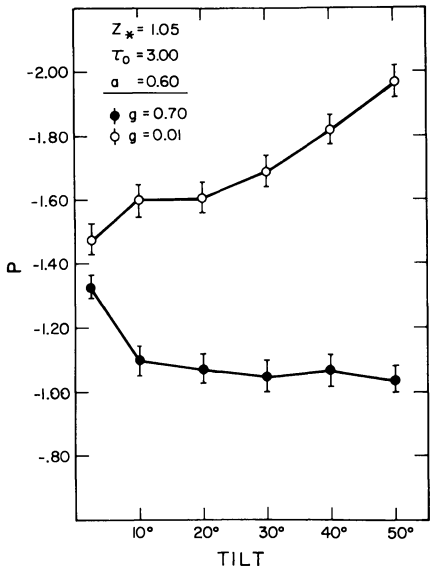

Fig. 12. Monte Carlo model calculations: The exponent of the surface brightness power law as a function of nebular tilt for the same model as Figure 11

decrease in the surface brightness at 800″ for the same change. The degree of this divergence and the value of the critical tilt probably depends on the specific shape of actual phase function of the nebular grains as well as on geometric factors such as the star's distance from the nebula and the thickness of the nebular sheet.

The principal conclusion, however, remains. The observations, as represented in Figure 5, can be explained if we assume that the Merope nebula is tilted with its southern, bright part toward the observer with a tilt angle well in excess of 50°. Simultaneously, the phase function asymmetry must change with wavelength in the sense that g may be near 0.7 at 5620 Å but decreases steadily as we progress toward shorter wavelengths. A further result of this would be the requirement that the actual perpendicular optical thickness τ_0 of the Merope nebula would only be of the order 0.5 or less at 5620 Å.

What is the effect of such a tilt with a wavelength variation of g in the indicated sense on the value of the power p of the surface brightness distribution? This is answered by Figure 12. The value of p for $g = 0.70$ does not change by more than 5% for tilt angles above 10°, whereas p increases by 20% for $g = 0.01$ as θ is increased from 10° to 50°. The way to achieve the observed large range of p is to assume a substantial tilt with the simultaneous decrease of g as the wavelength decreases. A more appropriate model for the Merope Nebula with $\tau_0 = 0.53$, $g = 0.75$, a tilt of 70°, and a star-front distance of 0.05 pc, shows the low value of $p = -0.59$, very close to the observed value at 5620 Å.

By careful adjustment of various model parameters detailed fits to the observations could certainly be achieved in the future. In Figure 13 we demonstrate how in a case of $\tau_0 = 2$ with $g = 0.70$ the values of p and $\log(S/F)$ depend on the star-nebula distance. Similar changes are expected when the physical thickness of the nebula is changed. In Figure 14 we show the change of the same quantities as function of the phase function asymmetry g for a star-nebula distance of 0.05 pc and $\tau_0 = 3$. Both figures are designed to illustrate the strong inter-relationship of all the parameters required to describe the problem.

In the light of our conclusions so far, can we explain the colour changes with distance discussed in Section II.4? We had seen that both an increase in optical depth with decreasing wavelength and a decrease of the phase function asymmetry lead to a steepening of the surface brightness distribution and consequently to a strong reddening of the nebular colour with increasing angular distance. This explanation would apply to the (2200–3300) colour which varies strongly with angular distance as is evident in Figure 6. However, if the wavelength dependence of optical depth follows the course found by Bless and Savage (1972), we should expect the optical depth to decline as we proceed from 2200 to 1550 Å. If the albedo and phase function were to remain constant through this spectral region, the (1550–2200) colour would actually become bluer with increasing angular distance. Since the opposite is observed in Figure 6, we must conclude, therefore, that g must continue to decline from 2200 to 1550 Å at a rate sufficient to reverse the colour trend caused by the decrease in optical depth. It is apparent from Figure 14 that the strong dependence of p on g continues down to $g = 0$. It can, therefore, not be ruled out that the phase function at 1550 Å is becoming entirely isotropic in nature or similar to a Rayleigh phase function. It will require more detailed modeling to determine the total range of decrease of g required to satisfy the observations from λ 5620 to λ 1550 Å. The data on Figure 6 also leave open the

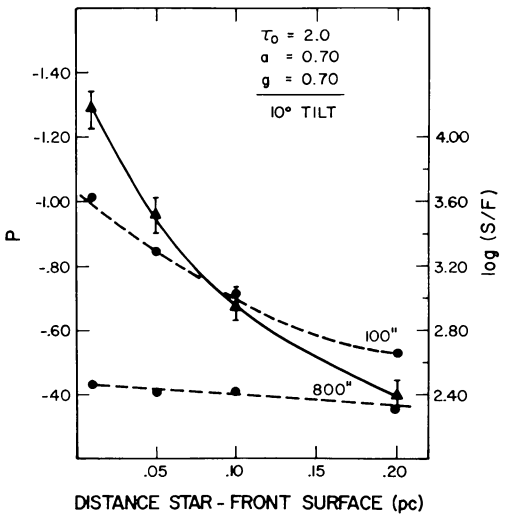

Fig. 13. Monte Carlo model calculations: The dependence of the relative surface brightness at 100″ and 800″ angular distance, and that of the exponent in the surface brightness power law is shown as function of the distance of the illuminating star from the front surface of the nebula. The optical depth $\tau_0=2$ and particles with $a=0.7$ and $g=0.7$ were chosen to illustrate the very general behavior

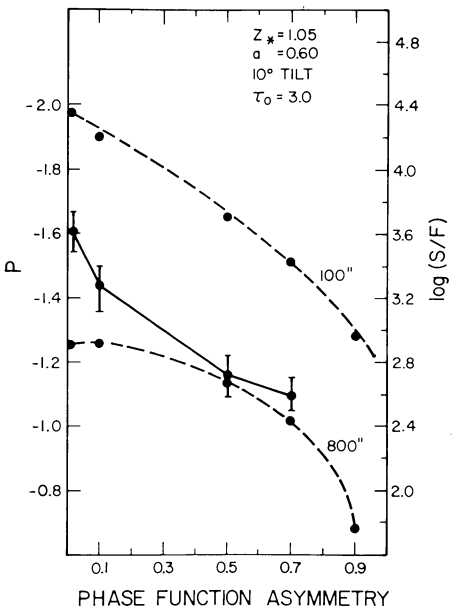

Fig. 14. Monte Carlo model calculations: The dependence of the relative surface brightness at 100″ and 800″ angular distance, and that of the exponent in the surface brightness power law is shown as function of the phase function asymmetry g

possibility of an albedo increase shortward of 2200 Å, raising its value above the already high level of albedo ($a>0.7$), which is required if the observations at the longer wavelengths are to be explained. It is not possible at this stage to reach a conclusion about the extent to which the wavelength dependence of the albedo of typical interstellar grains as found by Lillie and Witt (1976) applies to the grains in the Merope nebula. Effects due to possible albedo changes are relatively weak compared to changes introduced by variations in the phase function combined with geometric effects. Even a change by a factor of two in albedo causes the quantity $\log(S/F)$ to vary only by approximately ± 0.3 and produces a minor effect on p due to the influence of the albedo on the multiplicity of scattering.

IV. Conclusions

The measurements of the surface brightness of the Merope reflection nebula by the UV experiment of ANS have been shown to form a set of data highly consistent with existing ground-based observations of the same nebula by O'Dell (1965). The Monte Carlo technique of calculating the detailed radiative transfer has provided a successful approach to a qualitative understanding of the nebular observations. At this stage it cannot be excluded and in fact it appears likely that the illuminating star, 23 Tau, is located in front of the nebula at a distance to the surface of a few 10^{-2} pc. Despite substantial multiple scattering, which is increasing in importance with angular distance from the star, we find that *the change of the scattering phase function with wavelength* remains of *dominating influence* on the surface brightness distributions at different wavelengths. We conclude that the phase function must vary from a strongly forward throwing form at 5620 Å to a more nearly isotropic form at 1550 Å. One recalls that for wavelengths below 1800 Å the combination of high albedo and isotropic scattering is characteristic for 10 Å size radicals (Andriesse and de Vries, 1974). Even then, the strong reddening of the nebular colour at larger angular distances can only be realized if the principal nebula plane is tilted with respect to the plane of the sky by an amount exceeding 50°. It is our interpretation that the bright southern part of the Merope nebula is tilted toward the observer.

In the specific geometry of the Merope nebula the nebular light is largely backscattered radiation except at large angular distances to the south where some scattering at angles $\alpha<90°$ may be seen. Changes in the albedo with wavelength could be more than compensated for by very small variations in the phase function and would therefore go unrecognized. The solution to this problem would clearly lie in observations of similar detail as reported in this paper of another reflection nebula, where the illuminating star is deeply immersed in the nebula and where foreward scattering would prevail. Instead of counteracting each other, albedo and phase function changes would reinforce each other in such a situation.

Acknowledgements. The ANS project was sponsored by the Dutch Committee for Geophysics and Space Research of the Royal Netherlands Academy of Sciences. We acknowledge the cooperation of the ANS-UV team, Drs. J. W. G. Aalders, K. S. de Boer, R. J. van Duinen, D. Kester, P. R. Wesselius and C. C. Wu in scheduling the observations and in numerous discussions about the data reductions.

We received substantial grants of free computing time from the Los Alamos Scientific Laboratory through the helpful services of Dr.

Walter Huebner and we thank him for this assistance. Thanks are also due to Mr. D. E. Sprandel for his assistance with the model calculations at The University of Toledo. Material support for this study was provided by the U.S. National Aeronautics and Space Administration through grants No. NSG-7041 to The University of Toledo and NGR-06-003-176 to the University of Colorado.

References

Aalders, J. W. G.: 1976, ROG Note 76-2 on efficiencies
Allen, C. W.: 1973, Astrophysical Quantities, 3rd Ed., London: Athlone Press
Andriesse, C. D., de Vries, J.: 1974, *Astron. Astrophys.* **30**, 51
Bless, R. C., Savage, B. D.: 1972, *Astrophys. J.* **171**, 293
Code, A. D.: 1973, in IAU Symp. **52**, J. M. Greenberg and H. C. van de Hulst, Eds., Reidel, Dordrecht, p. 505
de Boer, K. S., Koornneef, J.: 1975, ROG Note 75-63 on background
Dahn, C.: 1967, Unpublished Ph. D. Thesis, Case Institute of Technology
Elvius, A., Hall, J. S.: 1966, *Lowell Observatory Bull. VI*, No. 135, 257
Fesenkov, V. G.: 1955, *Astron. Zh.* **32**, 97
FitzGerald, M. P., Stephens, T. C., Witt, A. N.: 1976, *Astrophys. J.*, in press
Greenberg, J. M., Hanner, M. S.: 1970, *Astrophys. J.* **161**, 947
Henyey, L. G., Greenstein, J. L.: 1941, *Astrophys. J.* **93**, 70
Lillie, C. F., Witt, A. N.: 1976, *Astrophys. J.*, in press
Maeder, A.: 1975, *Astron. Astrophys.* **42**, 471
Mattila, K.: 1970, *Astron. Astrophys.* **9**, 53
Mendoza, E. E.: 1965, *Bol. Obs. Tanantzintla y Tacubaya* **4**, 3
O'Dell, C. R.: 1965, *Astrophys. J.* **142**, 604
Roark, T., Roark, B., Collins, G. W., III: 1974, *Astrophys. J.* **190**, 67
Savage, B. D.: 1975, *Astrophys. J.* **199**, 92
van Duinen, R. J., Aalders, J. W. G., Wesselius, P. R., Wildeman, K. J., Wu, C. C., Luinge, W., Snel, D.: 1975, *Astron. Astrophys.* **39**, 159
Vanysek, V.: 1969, *Vistas in Astronomy* **11**, 189, ed. A. Beer, Oxford-Pergamon Press
Wesselius, P. R.: 1975, ROG Note 75-1 on calibration
Witt, A. N., Lillie, C. F.: 1973, *Astron. Astrophys.* **25**, 397
Witt, A. N.: 1976, in preparation